Nuclear Medicine and Molecular Imaging (2020) 54:233–240
https://doi.org/10.1007/s13139-020-00661-8

ORIGINAL ARTICLE

ISSN (print) 1869-3482
ISSN (online) 1869-3474

Comparison of Image Quality and Semi-quantitative Measurements with Digital PET/CT and Standard PET/CT from Different Vendors

Sung Hoon Kim [1,2] · Bong-Il Song [2] · Hae Won Kim [2] · Kyoung Sook Won [2]

Received: 22 May 2020 / Revised: 13 July 2020 / Accepted: 4 August 2020 / Published online: 13 August 2020

Abstract

Purpose This study aimed to evaluate the concordance and equivalence of results between the newly acquired digital PET/CT(dPET) and the standard PET/CT (sPET) to investigate possible differences in visual and semi-quantitative analyses.

Methods A total of 30 participants were enrolled and underwent a single ^{18}F-FDG injection followed by dual PET/CT scans, by a dPET scan, and immediately after by the sPET scan or vice versa. Two readers reviewed overall image quality using a 5-point scale and counted the number of suggestive ^{18}F-FDG avid lesions. The SUV values were measured in the background organs and in hypermetabolic target lesions. Additionally, we objectively evaluated image quality using the liver signal-to-noise ratio (SNR).

Results The dPET identified 4 additional ^{18}F-FDG avid lesions in 3 of 30 participants with improved visual image quality. The standard deviations of SUV of the background organs were significantly lower with Digital$_{PET}$ than with sPET, and dPET could acquire images with better SNR (11.13 ± 2.01 vs. 8.71 ± 1.32, $P < 0.001$). The reliability of SUV values between scanners showed excellent agreement. Bland-Altman plot analysis of 81 lesions showed an acceptable agreement between scanners for most of the SUVmax and SUVpeak values. No relationship between the SUV values and time delays of dual PET/CT acquisition was found.

Conclusions The dPET provides improved image quality and lesion detectability than the sPET. The semi-quantitative values of the two PET/CT systems of different vendors are comparable. This pilot study will be an important basis for possible interchangeable use of either system in clinical practice.

Keywords Digital PET · PET/CT · ^{18}F-FDG · SiPM · Silicon photomultiplier · Image quality

Introduction

Positron emission tomography/computed tomography (PET/CT) is a well-established functional imaging modality, with maximal applications in oncology (94%), cardiology (3%), and neurology (3%) [1]. Presently, the most commonly used tracer for PET/CT is ^{18}F-fluorodeoxyglucose (^{18}F-FDG), and ^{18}F-FDG PET/CT has become a popular method for detection, staging, restaging, and response evaluation in oncology [2].

Technical advances in PET instrumentation, in terms of photon sensitivity and spatial and timing resolutions, are expected to enhance detection capability, personalize therapeutic planning, and reduce the injection dose [3]. Recently, a digital PET/CT system with silicon photomultiplier (SiPM) detectors was developed and is expected to offer several benefits, including compact size, better intrinsic timing resolution, and a higher value of photon detection efficiency than that obtained by standard PET/CT system with photomultiplier tubes (PMTs) [1, 4].

Standardized uptake value (SUV) is being used routinely in oncological ^{18}F-FDG PET/CT examinations for tumor quantification [5]. The progressive wide-spread use of digital PET/CT will eventually raise the question of whether digital and

✉ Kyoung Sook Won
won@dsmc.or.kr

Sung Hoon Kim
sweetspirit3@naver.com

Bong-Il Song
song@dsmc.or.kr

Hae Won Kim
hwkim@dsmc.or.kr

[1] Department of Nuclear Medicine, Keimyung University Daegu Dongsan Hospital, Daegu, South Korea

[2] Department of Nuclear Medicine, Keimyung University Dongsan Hospital, Keimyung University School of Medicine, 1095 Dalgubeol-daero, Dalseo-gu, Daegu 42601, Republic of Korea

standard PET/CT systems can be used interchangeably for follow-up PET/CT studies, particularly for response assessment studies in oncological patients [6].

We recently installed a digital PET/CT scanner (Discovery MI; GE Healthcare, Milwaukee, WI, USA) at our institute in April 2019. Till date, no previous study has attempted to compare image quality and data of semi-quantitative measurements between digital and standard PET/CT systems from different vendors. Thus, this study aimed to evaluate the concordance and equivalence of results between the newly acquired digital PET/CT and the standard PET/CT (Biograph mCT; Siemens Healthineers, Knoxville, TN, USA) used in our hospital to investigate possible differences in qualitative and semi-quantitative analyses.

Materials and Methods

Participants

This prospective, single-center study was conducted between May and June 2019, and a total of 30 participants were enrolled and underwent a single ^{18}F-FDG injection and subsequently underwent a dual PET/CT scans—first, a digital PET/CT scan, and immediately thereafter, a standard PET/CT scan, or vice versa. All participants provided informed consent for their participation, and the study protocol was approved by Institutional Review Board of our hospital.

Imaging Protocol

All participants received a single ^{18}F-FDG injection for the dual PET/CT scans. The scans were performed with two different integrated PET/CT scanners. Before the ^{18}F-FDG injection, all patients fasted for at least 6 h, and a blood glucose level of < 150 mg/dL was maintained. The first PET/CT images were acquired 60 min after the ^{18}F-FDG injection; the second PET/CT scan was performed immediately after the first scan. Fifteen participants underwent a digital PET/CT scan first and a standard PET/CT thereafter; the remaining 15 patients underwent scanning in the reverse order to control for the changes in metabolic activity and image quality.

First, a low-dose CT scan was acquired for attenuation correction and anatomic localization, without any oral or intravenous contrast agent. The CT acquisition parameters for both scanners were as follows: peak voltage of 120 kVp, automated exposure control using CARE Dose4D, and slice thickness of 3.0 mm for standard PET/CT (Biograph mCT) or peak voltage of 120 kVp, automated tube current ranging from 10 to 50 mA using Smart mA, and slice thickness of 2.8 mm for digital PET/CT (Discovery MI). Immediately after the CT scan, PET scan was obtained with an acquisition time of 1.5 min/bed position for both PET/CT systems in three-dimensional mode. The standard PET images were reconstructed using an ordered subset expectation maximization (OSEM) iterative algorithm with both time-of-flight (TOF) and point-spread function (PSF) recovery, the so-called ultraHD·PET, with 2 iterations and 21 subsets in 256 matrix size. The digital PET images were reconstructed using VUE Point FX with Sharp IR (OSEM + TOF + PSF) in 256 matrix size, with application of Bayesian penalized likelihood (Q.Clear®) reconstruction (β value of 600). Both PET images were reconstructed using locally preferred, clinically relevant, and vendor-recommended protocols.

Image Analysis

Two board-certified interpreters reviewed the 2 sets of PET/CT images using AW Server 3.2 (GE Healthcare); each image set was graded visually and subjectively based on 5-point Likert scales ranging from 1 to 5 (1 = non-diagnostic to 5 = excellent diagnostic), and the readers counted the number of suggestive ^{18}F-FDG avid lesions. For semi-quantitative analysis, the SUVs were measured in the two different background organs (liver and blood pool) and in up to four ^{18}F-FDG avid lesions per each patient. A 3-cm-diameter spherical volume of interest (VOI) was drawn on normal right hepatic parenchyma, and 2-cm-diameter spherical VOI was placed on aortic arch (blood pool) to obtain the background SUVs. The mean SUV (SUVmean), maximum SUV (SUVmax), and standard deviation (SD) were obtained for background activity. The liver signal-to-noise ratio (SNR) was recorded as a quantitative parameter of image quality; SNR was calculated as the ratio of SUVmean to SD in the liver VOI. The SUVmax and peak SUV (SUVpeak) were used for measuring the ^{18}F-FDG avid lesions.

Statistical Analysis

Numeric data are expressed as mean ± SD. The paired Student *t* test was performed to compare the visual scoring of image quality and SUV values acquired on the two PET/CT scanners. An equivalence test was performed on each of the background organs and target lesions with an equivalence interval of [− 0.7, 0.7] [7]. The inter-rater agreement for visual image quality assessment was evaluated using the kappa statistic. Reliability of SUV values between the two scanners was measured using the intraclass correlation coefficient (ICC) and is reported as estimates with a 95% confidence interval (CI). Bland-Altman plots were generated to assess the agreement between the two scanners. The relation between different SUV values and time delay between scans was evaluated by using partial correlation and linear regression analysis.

All statistical analyses were performed using MedCalc for Windows, version 19.1.7 (MedCalc Software, Ostend, Belgium) and R version 3.4.3 software (http://www.r-

project.org, R Foundation for Statistical Computing, Vienna, Austria). All P values < 0.05 were considered statistically significant.

Results

A total of 30 participants (11 men and 19 women; 28 for oncological examination and 2 for health screening; mean age, 63.0 ± 11.4 years) were enrolled. The dose of injected ^{18}F-FDG was 5.60 ± 0.86 mCi (range, 4.27–7.76). The first PET/CT scans acquired 61.5 ± 5.4 min after ^{18}F-FDG injection. The mean time delay between both scans was 17.6 ± 5.3 min. The demographic and clinical information of the enrolled patients are listed in Table 1.

Images acquired by digital PET/CT had significantly higher visual scoring than that acquired by standard PET/CT (4.90 ± 0.30 vs. 4.28 ± 0.45, $P < 0.0001$), with moderate inter-reader agreement and a weighted kappa of 0.49 (95% CI, 0.27–0.71). The digital PET/CT system could identify 4 additional ^{18}F-FDG avid lesions in 3 of 30 participants.

Table 2 shows the SUV values of the background organs and target lesions. The SD of the background organs was significantly lower with digital PET/CT than those with standard PET/CT (liver SD, 0.21 ± 0.06 vs. 0.27 ± 0.09, $P < 0.001$; blood pool SD, 0.17 ± 0.04 vs. 0.19 ± 0.06, $P = 0.048$), and the SNR obtained by digital PET/CT was higher than that obtained by standard PET/CT (11.13 ± 2.01 vs. 8.71 ± 1.32, $P < 0.001$). The mean values of SUVmax and SUVmean of 30 background organs, as well as the SUVmax and SUVpeak of 81 target lesions, showed no significant

Table 1 Demographic and clinical data of 30 study participants

Patient no.	Age (years)	Sex	Weight (kg)	Disease	Injected ^{18}F-FDG dose (mCi)	First acquisition PET/CT	Start Time (min)	Time delay (min)
1	81	F	36	Thyroid cancer	4.27	Standard	60	28
2	50	M	78	Cancer screening	6.11	Standard	68	35
3	77	F	58	Breast cancer	5.43	Digital	60	18
4	61	M	62	Lung cancer	5.76	Digital	59	21
5	54	F	55	Liposarcoma	5.30	Standard	62	20
6	72	M	61	Stomach cancer	6.38	Standard	56	13
7	39	F	70	Cervical cancer	6.43	Digital	57	16
8	73	M	54	Stomach cancer	5.08	Digital	62	22
9	57	F	50	Breast cancer	4.96	Digital	55	15
10	44	F	49	Thyroid cancer	5.76	Standard	56	13
11	55	F	61	Breast cancer	6.00	Standard	63	13
12	76	M	65	Colon cancer	6.92	Digital	55	20
13	50	F	53	GIST	5.38	Standard	63	14
14	58	F	42	Breast cancer	5.05	Standard	60	14
15	69	M	61	Lung cancer	5.78	Digital	73	21
16	62	F	56	Lung cancer	6.22	Digital	70	20
17	73	F	43	Breast cancer	5.11	Digital	66	23
18	81	F	47	Cervical cancer	4.70	Digital	65	27
19	65	M	48	Esophageal cancer	4.78	Standard	68	15
20	61	F	66	Cancer screening	5.27	Standard	62	12
21	72	F	36	Cervical cancer	4.32	Digital	63	15
22	39	F	55	Cervical cancer	5.73	Digital	54	14
23	61	F	59	Lung cancer	6.05	Digital	56	17
24	67	M	64	Lung cancer	6.19	Digital	69	14
25	59	F	55	Cervical cancer	5.65	Standard	55	13
26	68	M	54	Lung cancer	6.70	Standard	70	14
27	65	M	65	Lymphoma	5.43	Digital	56	17
28	59	F	81	Breast cancer	7.76	Standard	63	17
29	77	M	63	Colon cancer	5.92	Standard	54	16
30	64	F	56	Tongue cancer	4.76	Standard	64	12

GIST, gastrointestinal stromal tumor

Table 2 Summary of SUV parameters in the background organs and target lesions

SUV parameter	Digital PET/CT	Standard PET/CT	*P*	Difference	90% CI	Equivalence level
Liver SUVmax	3.09 ± 0.68	3.20 ± 0.71	0.068	0.11 ± 0.31	0.011; 0.205	Equivalent
Liver SUVmean	2.31 ± 0.44	2.31 ± 0.43	0.811	0.01 ± 0.21	− 0.056; 0.075	Equivalent
Liver SUVsd	0.21 ± 0.06	0.27 ± 0.09	< 0.001	0.06 ± 0.05	0.046; 0.077	
Blood pool SUVmax	2.09 ± 0.43	2.07 ± 0.44	0.753	− 0.02 ± 0.39	− 0.146; 0.100	Equivalent
Blood pool SUVmean	1.58 ± 0.36	1.54 ± 0.33	0.299	− 0.04 ± 0.27	− 0.124; 0.046	Equivalent
Blood pool SUVsd	0.17 ± 0.04	0.19 ± 0.06	0.048	0.02 ± 0.06	0.004; 0.043	
Lesions SUVmax	7.72 ± 7.30	7.58 ± 8.40	0.532	− 0.14 ± 2.05	− 0.522; 0.236	Equivalent
Lesions SUVpeak	5.27 ± 6.02	5.07 ± 5.99	0.089	− 0.19 ± 1.02	− 0.383; − 0.006	Equivalent
SNR	11.13 ± 2.01	8.71 ± 1.32	< 0.001	− 2.42 ± 1.98	− 3.031; − 1.801	

Data are presented as mean with standard deviation

SUV, standardized uptake value; *CI*, confidence interval; *SUVmax*, maximum SUV; *SUVmean*, mean SUV; *SUVsd*, standard deviation of SUV; *SUVpeak*, peak SUV; *SNR*, signal-to-noise ratio of the liver

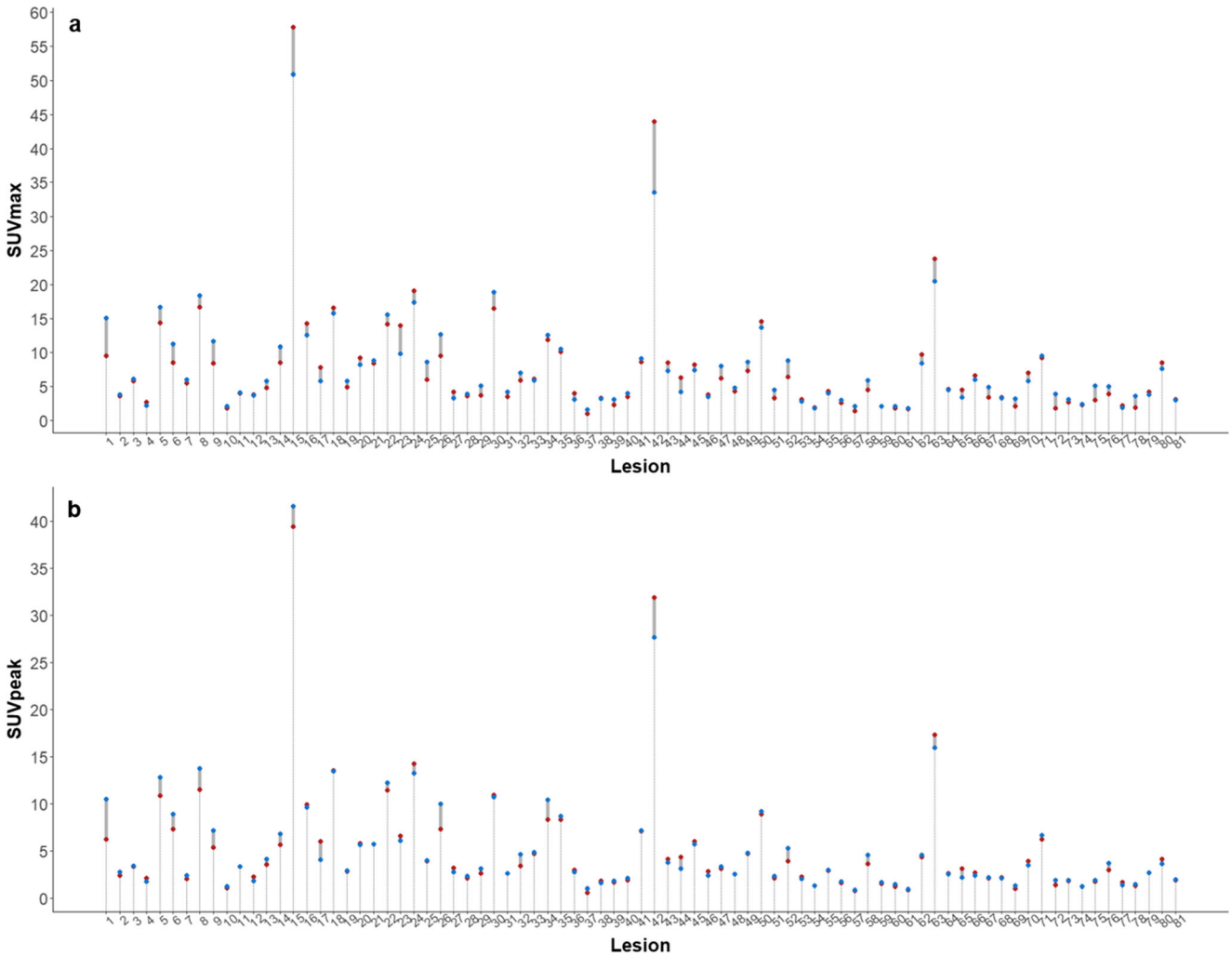

Fig. 1 Per-lesion differences in SUVmax (**a**) and SUVpeak (**b**) between two scanners (blue dot, digital PET/CT; red dot, standard PET/CT)

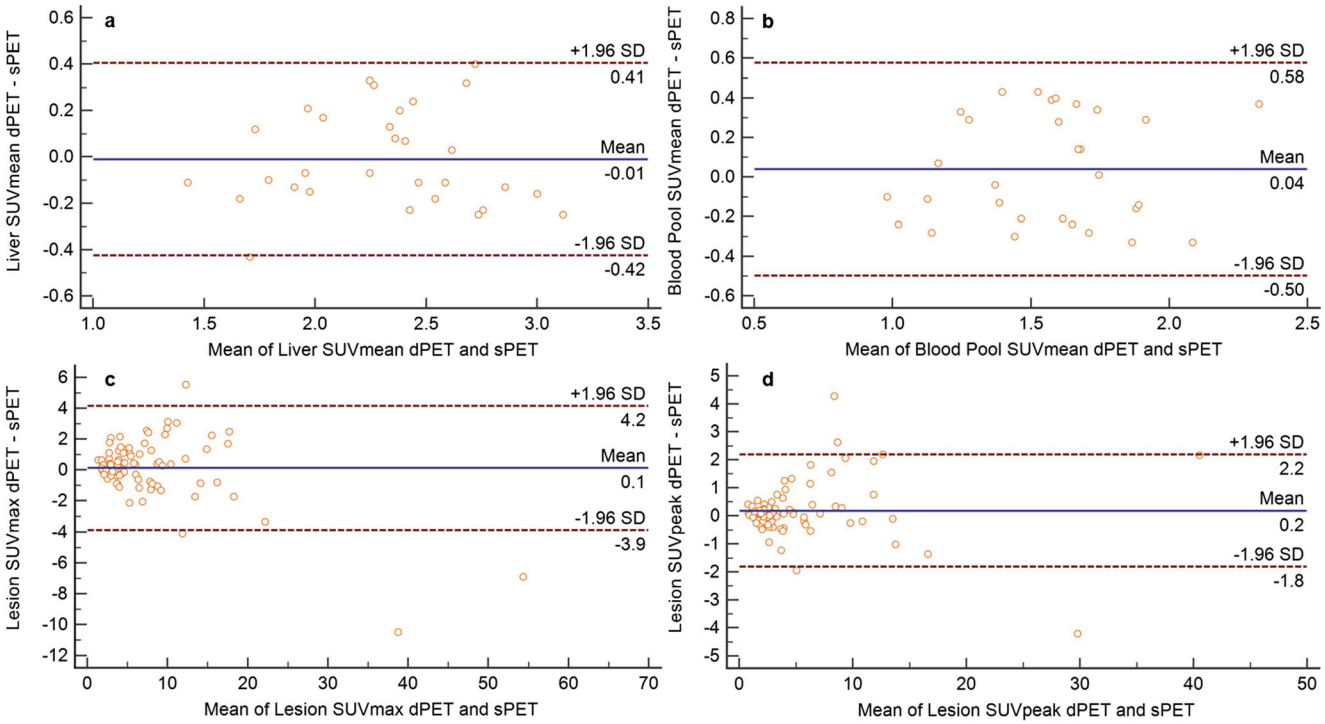

Fig. 2 Bland-Altman plots of digital and standard PET/CT plotted against averages of the liver SUVmean (**a**), blood-pool SUVmean (**b**), lesion SUVmax (c), and lesion SUVpeak (**d**)

difference. Equivalence was achieved for all background organs and target lesions matched per patient.

The reliability of SUV values between scanners showed excellent agreement; ICCs of the liver SUVmax, liver SUVmean, lesion SUVmax, and SUVpeak were 0.947 (0.888–0.975), 0.937 (0.869–0.970), 0.983 (0.973–0.989), and 0.993 (0.989–0.995). Differences in SUV values in each target lesion are shown in Fig. 1.

Analysis of the Bland-Altman plots for 81 lesions shows an acceptable agreement between scanners for most of the registered SUVmax and SUVpeak values (Fig. 2). Additionally, very good agreement was observed between the two PET/CT systems for liver SUVmean, blood pool SUVmean, target lesion SUVmax, and SUVpeak.

No relationship between the target lesion SUV values and time delays of dual PET/CT acquisition is found in the linear regressions of SUVmax ($r = 0.14$; $P = 0.206$, Fig 3a) and SUVpeak ($r = 0.00$; $P = 0.993$, Fig. 3d) in a total of 30 participants. There also showed no statistical significance in the separate analyses according to dual PET/CT acquisition order (Fig. 3b, c, e, and f).

Discussion

The state-of-the-art SiPM PET technology can provide improved detection capability by high-definition visualization, fast acquisition times, and/or low-dose imaging or advanced quantitative precision [8, 9]. In comparison with standard PET, the higher detection sensitivity of digital PET is because of the different scintillator element coupling technology. Multiple PMTs are matched to multiple detectors in the standard PET system, whereas one-to-one correspondence (1:1 coupling) is achieved in the digital PET system, and each digital photon-counting detector includes thousands of avalanche photodiodes [1]. The superior timing and spatial resolution of digital PET system can be explained by the incorporation of these technologies with further improved the TOF performance over the standard PET system [6, 10].

In the current study, we assessed possible differences in both qualitative and semi-quantitative measurements between digital and standard PET/CT systems from different vendors. Our results demonstrate that digital PET/CT systems provide improved image quality than standard PET/CT system. Notably, these improvements are easily noticeable on a subjective visual assessment and could be scored visually; we find 4 additional ^{18}F-FDG avid target lesions in 3 of 30 participants with digital PET/CT scanner (Fig. 4). These findings are consistent with that reported in previously published studies. Nguyen et al. [8] reported that additional 8 lesions were detected with digital PET/CT in 5 of 21 patients. More recently, Sluis et al. [11] reported findings of additional ^{18}F-FDG-avid lesion, which resulted in upstaging disease, demonstrating the improved image quality obtained by digital PET/CT.

In addition, we objectively evaluated image quality using SNR. It has been used as a metric to assess the quality of

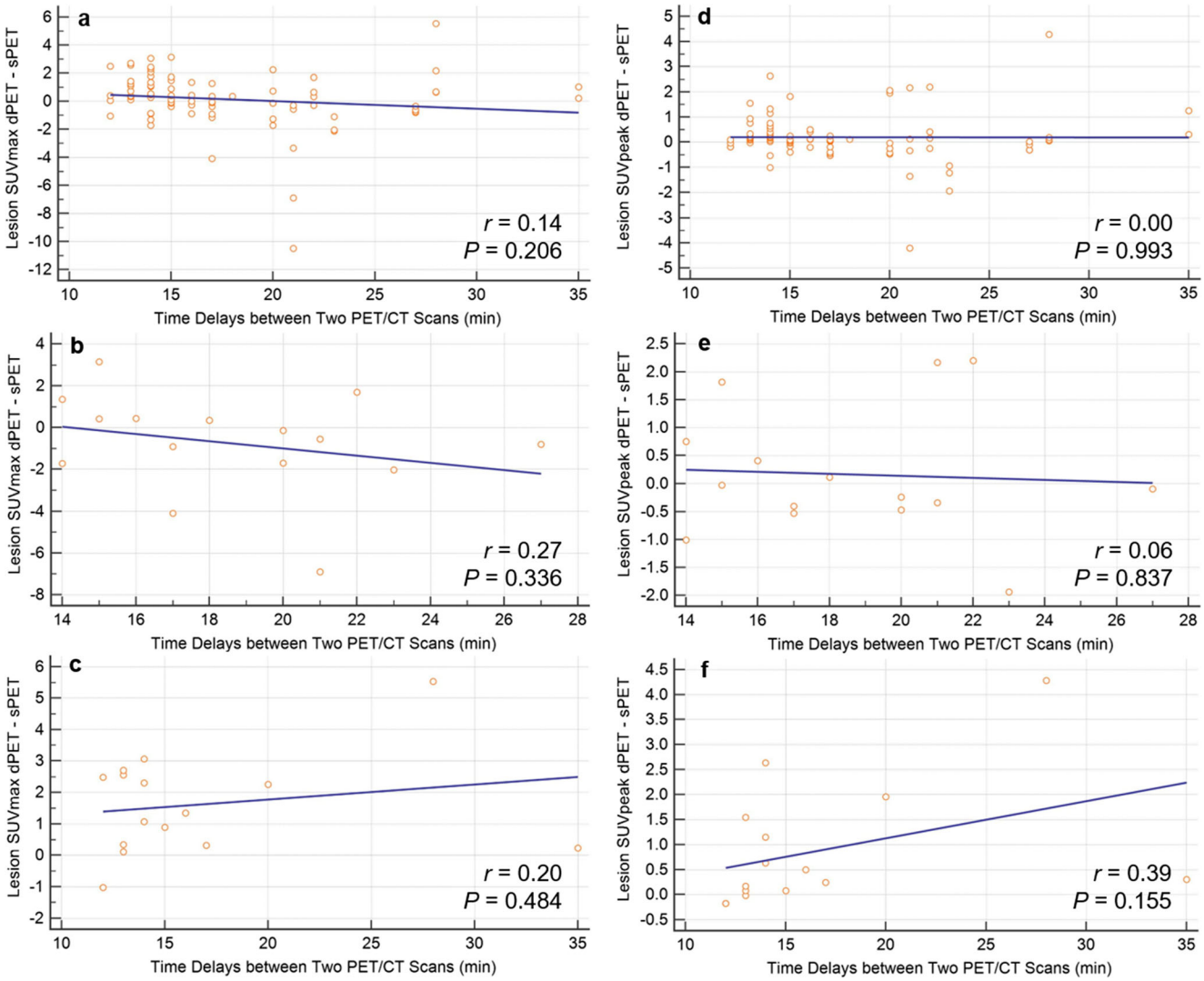

Fig. 3 Relationship between acquisition time delays and target lesion SUV values. **a** SUVmax in total of 30 participants, **b** SUVmax in participants with digital PET first, **c** SUVmax in participants with standard PET first, **d** SUVpeak in total of 30 participants, **e** SUVpeak in participants with digital PET first, and **f** SUVpeak in participants with standard PET first

reconstructed PET/CT images [12]. In this study, we used liver as the reference region because it has been widely used to quantitatively evaluate the quality of ^{18}F-FDG PET images because of its relatively homogenous uptake [13]. As shown in Table 2, digital PET/CT could acquire images with better SNR. To our knowledge, this is the first study to evaluate the quality of digital PET images using objective metric (e.g., SNR) compared with standard PET images. It should be considered that the application of the Q.clear® algorithm may have contributed to allow noise reduction [14]. A recent study of Messerli et al. [15] demonstrated that Q.clear® with β value of 600, as same value set in our study, leads to an increased subjective image quality with SNR in 45 patients with lung cancer.

Although most of the SUV parameters, except SD and SNR, showed no significant differences, our results obtained using the equivalence test demonstrated similar ^{18}F-FDG uptake in both the background organs and target lesions with two different PET/CT systems. This finding suggests the possible interchangeability of SUV values of either PET/CT scanner. In general, SUV is a highly reproducible imaging biomarker that is ideally suited for monitoring tumor response to treatment in individual patients; moreover, all variable SUV values (SUVmax, SUVmean, and SUVpeak) showed similar repeatability despite different tumor sampling approaches [16]. Particularly, in hospitals where both digital and standard PET/CT devices are installed, SUV values might be used interchangeably for follow-up studies of oncologic patients in busy clinical practice workflows. Further large-scale prospective studies are needed to validate the interchangeable use and repeatability of semi-quantitative parameters between the two different PET/CT systems.

The distribution time of ^{18}F-FDG affects the intensity of radiotracer accumulation and its clearance from the blood [17]. Two recent studies assessed the association of SUV values and time delays between digital and standard PET/CT

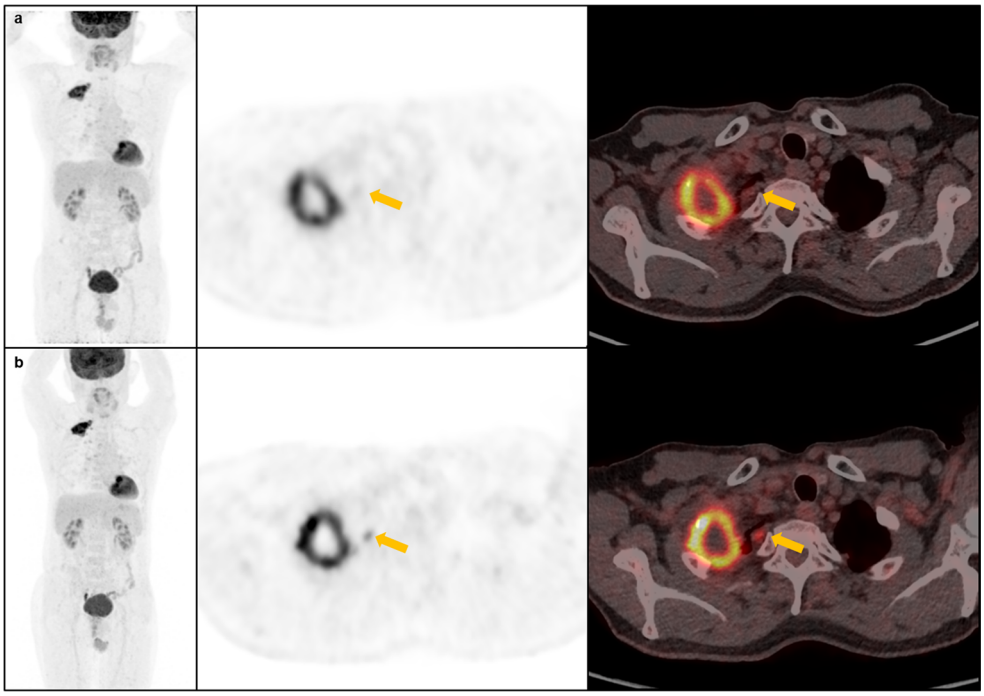

Fig. 4 Representative MIP, axial PET and fusion PET/CT images (from left to right) acquired on the standard PET/CT (**a**, upper row) and digital PET/CT (**b**, lower row) of a 68-year-old male patient with lung cancer. A small pleural lesion (yellow arrows) found on digital PET/CT that did not appear as such on standard PET/CT images

systems in controlled scan sequences, and they reported no significant influence or only limited association [6, 11]. Similarly, our results demonstrated no significant association between target lesion SUV values and time delays of dual PET/CT acquisition, although the trends of delayed SUV increase are noted especially in cases that underwent standard PET/CT first. In this study, the mean time delays (17.6 ± 5.3 min) were much shorter than that in the previous studies. No statistically significant differences in SUV parameters might be partially explained by short time delays and the strict balance between the dual PET/CT scan sequences.

The present study has a few limitations. The impossibility of acquiring dual PET/CT scans in the same time would have affected delayed increased uptake of target lesions and SUV values, although time delay between two scans was adjusted as short as possible. We also acknowledge the relatively small participant dataset with various primary malignancies. Further investigations with homogenous patient groups should be conducted to assess the potential benefits of digital PET/CT over standard PET/CT. The increasing use of digital PET/CT technology enables the opportunity to advance molecular imaging capabilities, supports personalized nuclear medicine, and bolsters the role of PET/CT beyond the field of oncology [18].

Conclusion

The present study identified that digital PET/CT provides better image quality than the standard PET/CT, including both observative improvement and significantly lower SNR. With respect to the semi-quantitative analysis, the SUV parameters obtained by the two different PET/CT systems are comparable. We believe this pilot study will be an important basis for interchangeable use of either system. Further studies will validate its possibility in real clinical practice.

Acknowledgments We thank the members of the Department of Nuclear Medicine, Keimyung University Dongsan Hospital for their dedicated support.

Compliance with Ethical Standards

Conflict of Interest Sung Hoon Kim, Bong-Il Song, Hae Won Kim, and Kyoung Sook Won declare that they have no conflict of interest.

Ethical Statement This study procedure followed the medical research protocols and ethics guidelines defined by the World Medical Association's Declaration of Helsinki throughout the study.

Informed Consent Informed consent was obtained from all individual participants included in this prospective study, approved by the local Institutional Review Board (2019-03-052).

References

1. Slomka PJ, Pan T, Germano G. Recent advances and future Progress in PET instrumentation. Semin Nucl Med. 2016;46:5–19.
2. Boellaard R, Delgado-Bolton R, Oyen WJG, Giammarile F, Tatsch K, Eschner W, et al. FDG PET/CT: EANM procedure guidelines for tumour imaging: version 2.0. Eur J Nucl Med Mol Imaging. 2015;42:328–54.

3. Hsu DFC, Ilan E, Peterson WT, Uribe J, Lubberink M, Levin CS. Studies of a next-generation silicon-photomultiplier-based time-of-flight PET/CT system. J Nucl Med. 2017;58:1511–8.
4. Wagatsuma K, Miwa K, Sakata M, Oda K, Ono H, Kameyama M, et al. Comparison between new-generation SiPM-based and conventional PMT-based TOF-PET/CT. Physica Medica. 2017;42: 203–10.
5. Kinahan PE, Fletcher JW. PET/CT standardized uptake values (SUVs) in clinical practice and assessing response to therapy. Semin Ultrasound CT MR. 2010;31:496–505.
6. Fuentes-Ocampo F, López-Mora DA, Flotats A, Paillahueque G, Camacho V, Duch J, et al. Digital vs. analog PET/CT: intra-subject comparison of the SUVmax in target lesions and reference regions. Eur J Nucl Med Mol Imaging. 2019;46:1745–50.
7. Baratto L, Park SY, Hatami N, Davidzon G, Srinivas S, Gambhir SS, et al. 18F-FDG silicon photomultiplier PET/CT: a pilot study comparing semi-quantitative measurements with standard PET/CT. PLoS One. 2017;12:e0178936.
8. Nguyen NC, Vercher-Conejero JL, Sattar A, Miller MA, Maniawski PJ, Jordan DW, et al. Image quality and diagnostic performance of a digital PET prototype in patients with oncologic diseases: initial experience and comparison with analog PET. J Nucl Med. 2015;56:1378–85.
9. Wright CL, Binzel K, Zhang J, Knopp MV. Advanced functional tumor imaging and precision nuclear medicine enabled by digital PET technologies. Contrast Media Mol Imaging. 2017;2017: 5260305.
10. López-Mora DA, Flotats A, Fuentes-Ocampo F, Camacho V, Fernández A, Ruiz A, et al. Comparison of image quality and lesion detection between digital and analog PET/CT. Eur J Nucl Med Mol Imaging. 2019;46:1383–90.
11. van Sluis J, Boellaard R, Somasundaram A, van Snick PH, Borra RJH, Dierckx RAJO, et al. Image quality and semiquantitative measurements on the biograph vision PET/CT system: initial experiences and comparison with the biograph mCT. J Nucl Med. 2020;61:129–35.
12. Amakusa S, Matsuoka K, Kawano M, Hasegawa K, Ouchida M, Date A, et al. Influence of region-of-interest determination on measurement of signal-to-noise ratio in liver on PET images. Ann Nucl Med. 2018;32:1–6.
13. Yan J, Schaefferkoette J, Conti M, Townsend D. A method to assess image quality for low-dose PET: analysis of SNR, CNR, bias and image noise. Cancer Imaging. 2016;16:26.
14. Caribé PRRV, Koole M, D'Asseler Y, Van Den Broeck B, Vandenberghe S. Noise reduction using a Bayesian penalized-likelihood reconstruction algorithm on a time-of-flight PET-CT scanner. EJNMMI Phys. 2019;6:22.
15. Messerli M, Stolzmann P, Egger-Sigg M, Trinckauf J, D'Aguanno S, Burger IA, et al. Impact of a Bayesian penalized likelihood reconstruction algorithm on image quality in novel digital PET/CT: clinical implications for the assessment of lung tumors. EJNMMI Phys. 2018;5:27.
16. Lodge MA. Repeatability of SUV in oncologic 18F-FDG PET. J Nucl Med. 2017;58:523–32.
17. Houshmand S, Salavati A, Segtnan EA, Grupe P, Høilund-Carlsen PF, Alavi A. Dual-time-point imaging and delayed-time-point fluorodeoxyglucose-PET/computed tomography imaging in various clinical settings. PET Clin. 2016;11:65–84.
18. Schillaci O, Urbano N. Digital PET/CT: a new intriguing chance for clinical nuclear medicine and personalized molecular imaging. Eur J Nucl Med Mol Imaging. 2019;46:1222–5.